A thermal boundary control method for a flexible thin disk rotating over critical and supercritical speeds

Yong-Chen Pei, Chris Chatwin, Ling He, Wen-Zuo Li

Publication date
07-01-2017

Document Version
Accepted version

Published in
Meccanica

Link to external publisher version
https://doi.org/10.1007/s11012-016-0418-y

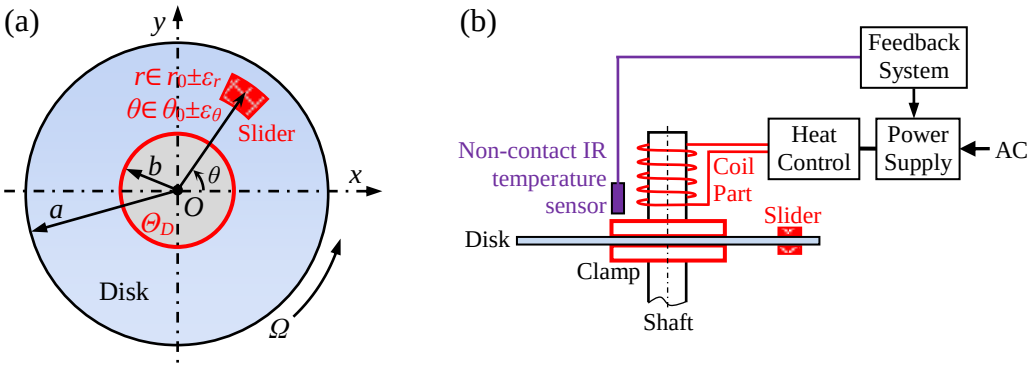

Fig.1 (a) A schematic diagram of the rotating disk subjected to a stationary slider loading system; (b) Thermal boundary feedback control schema using an induction coil to heat the drive shaft.

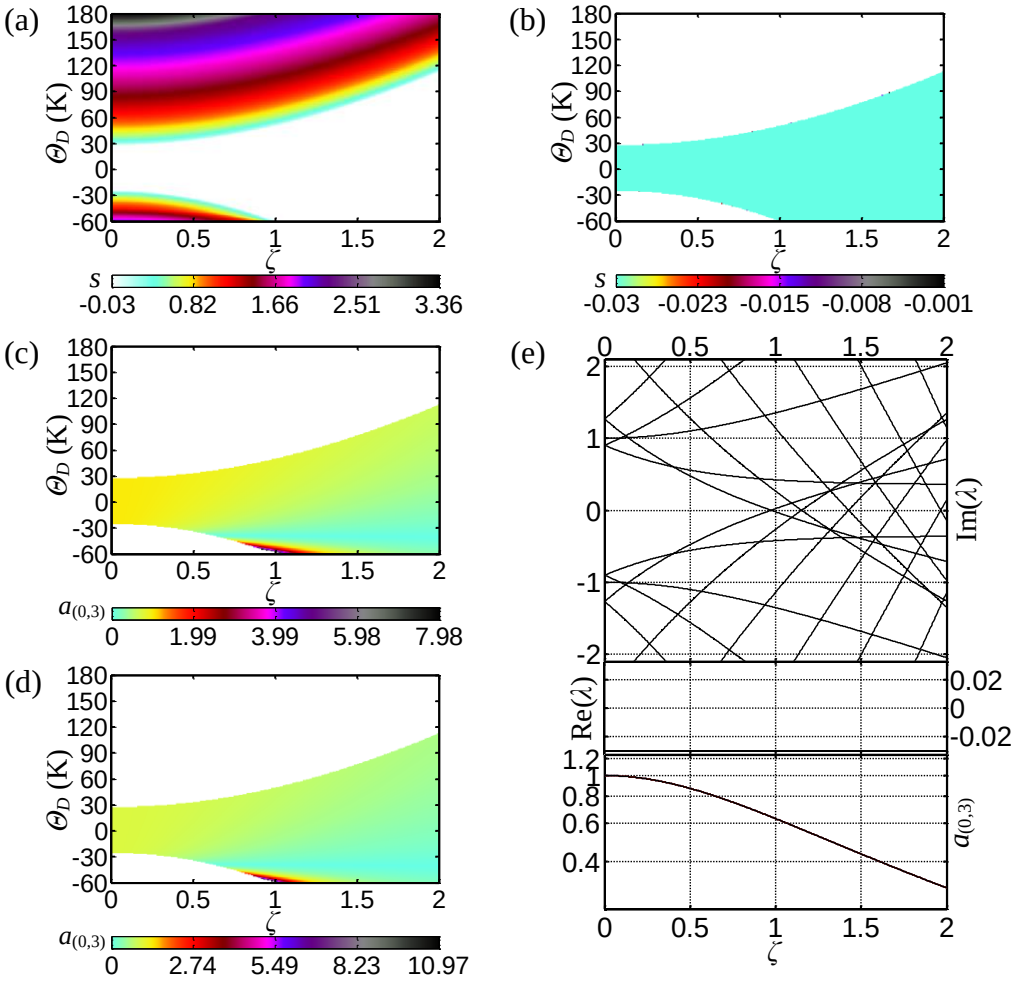

Fig.2 Dynamic characteristics of the rotating disk using shaft temperature increments for the case of slider mass m_s=0, disk air lift force χ=0 and slider spring initial deformation κ_F=0. (a) Dynamic stability on the dimensionless disk rotational speed ζ - for shaft temperature increments Θ_D, ζ-Θ_D plane; (b) Stable region on ζ-Θ_D plane; (c) Steady state amplitude $a_{(0,3)}$ on ζ-Θ_D plane: radial position r_P at slider radial center r_0; (d) Steady state amplitude $a_{(0,3)}$ on ζ-Θ_D plane: r_P at disk outer edge a; (e) Eigenvalue λ and $a_{(0,3)}$ without temperature control: r_P at disk outer edge a.

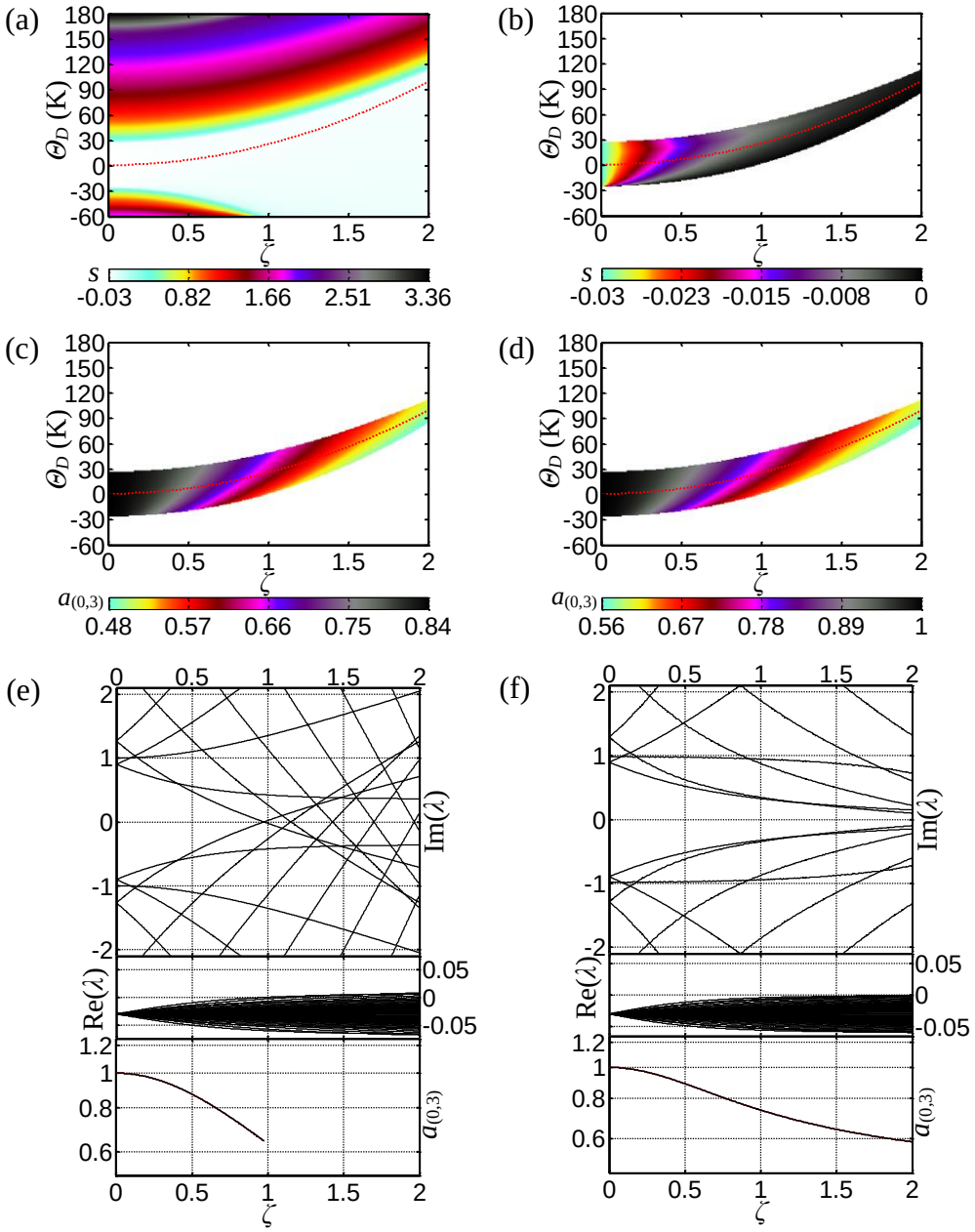

Fig.3 Dynamic characteristics of the rotating disk using shaft temperature increments for the case of slider mass m_s=0, disk air lift force χ=0.03 and slider spring initial deformation κ_F=0. (a) Dynamic stability on the dimensionless disk rotational speed ζ - for shaft temperature increments Θ_D, ζ-Θ_D plane; (b) Stabilized region on ζ-Θ_D plane; (c) Steady state amplitude $a_{(0,3)}$ on ζ-Θ_D plane: radial position r_P at slider radial center r_0; (d) Steady state amplitude $a_{(0,3)}$ on ζ-Θ_D plane: r_P at disk outer edge a; (e) Eigenvalue λ and $a_{(0,3)}$ without temperature control; (f) Eigenvalue λ and $a_{(0,3)}$ under shaft temperature increment control $\underline{\Theta_D}(\zeta)$. In (a-d), Red dotted line: the assigned shaft temperature increment control $\underline{\Theta_D}(\zeta)$. In the lowest subplot of (e-f), black line $a_{(0,3)}$: r_P at disk outer edge a.

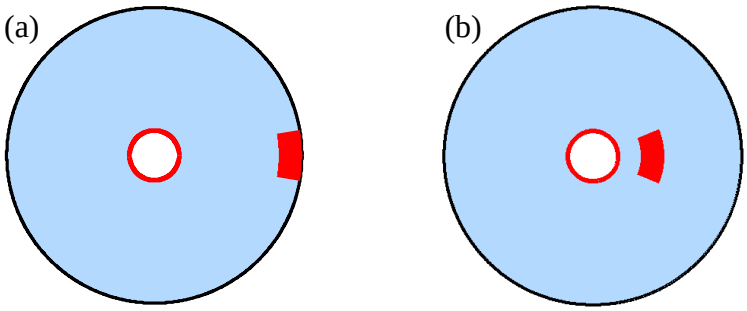

Fig.4 Two disk/slider configurations of a rotating disk subjected to a stationary slider loading system. Slider circumferential center θ_0=0, disk/slider interface radial length ε_r=15h and circumferential length ε_θ =2ε_r/r_0. (a) slider radial center r_0=a-ε_r; (b) slider radial center r_0=b+(a-b)/4.

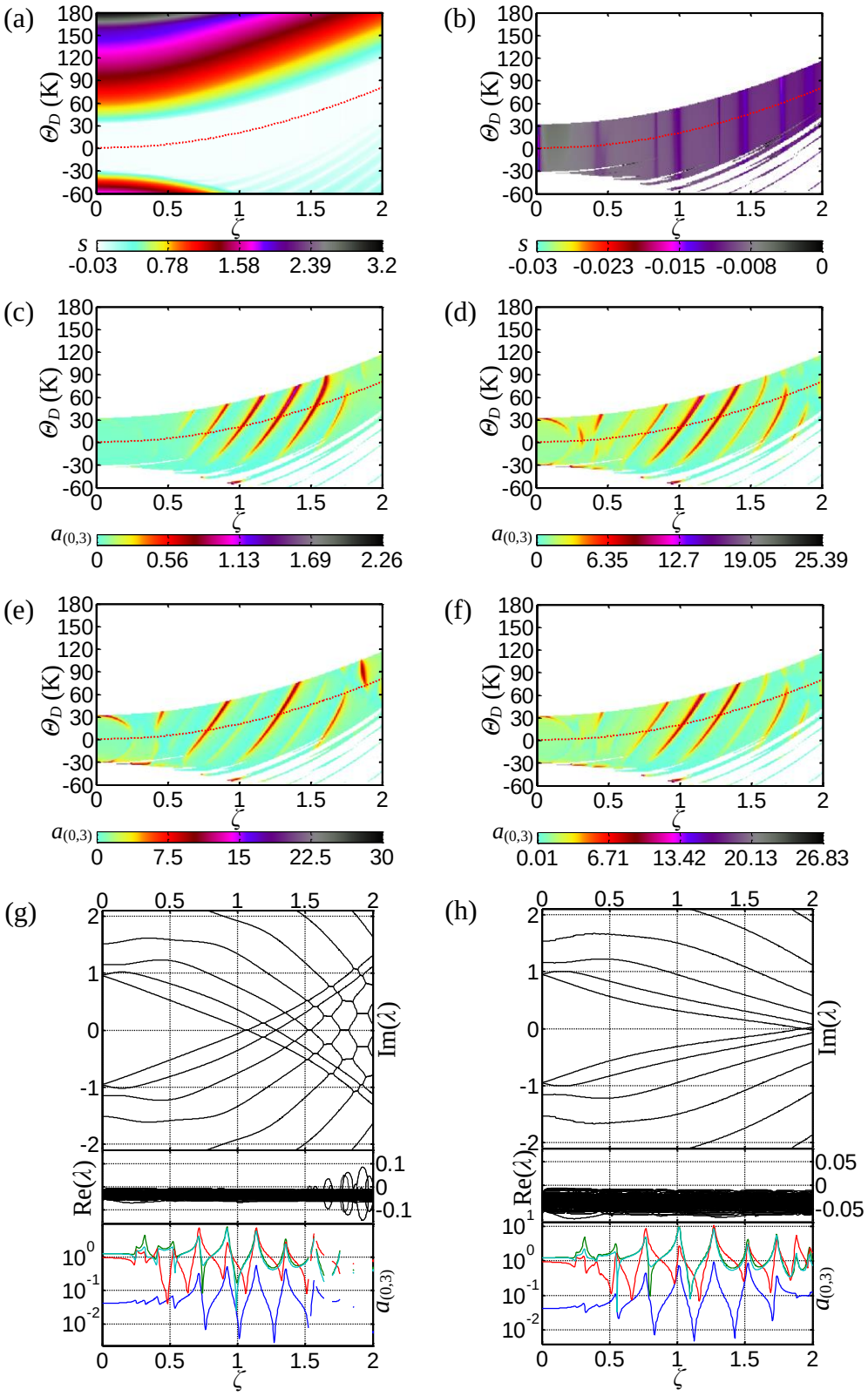

Fig.5 Dynamic characteristics of the rotating disk using shaft temperature increments for the case of slider mass m_s=0.01, disk air lift force χ=0 and slider spring initial deformation κ_F=0. Disk/slider configuration: Fig. 4(a). (a) Dynamic stability of the dimensionless disk rotational speed ζ - for shaft temperature increments Θ_D, ζ-Θ_D plane; (b) Stabilized region on ζ-Θ_D plane; (c) Steady state amplitude

$a_{(0,3)}$ on ζ-Θ_D plane: radial position r_P at disk outer edge a, circumferential position θ_P=0°; (d) $a_{(0,3)}$: r_P=a, θ_P=90°; (e) $a_{(0,3)}$: r_P=a, θ_P=180°; (f) $a_{(0,3)}$: r_P=a, θ_P=270°; (g) Eigenvalue λ and $a_{(0,3)}$ without temperature control; (h) Eigenvalue λ and $a_{(0,3)}$ with shaft temperature increment control $\underline{\Theta_D}(\zeta)$. In (a-f), Red dotted line: the assigned shaft temperature increment control $\underline{\Theta_D}(\zeta)$. In the nethermost subplot of (g-h), Blue line $a_{(0,3)}$: radial position r_P at disk outer edge a, circumferential position θ_P=0°; Green line $a_{(0,3)}$: r_P=a, θ_P=90°; Red line $a_{(0,3)}$: r_P=a, θ_P=180°; Cyan line $a_{(0,3)}$: r_P=a, θ_P=270°.

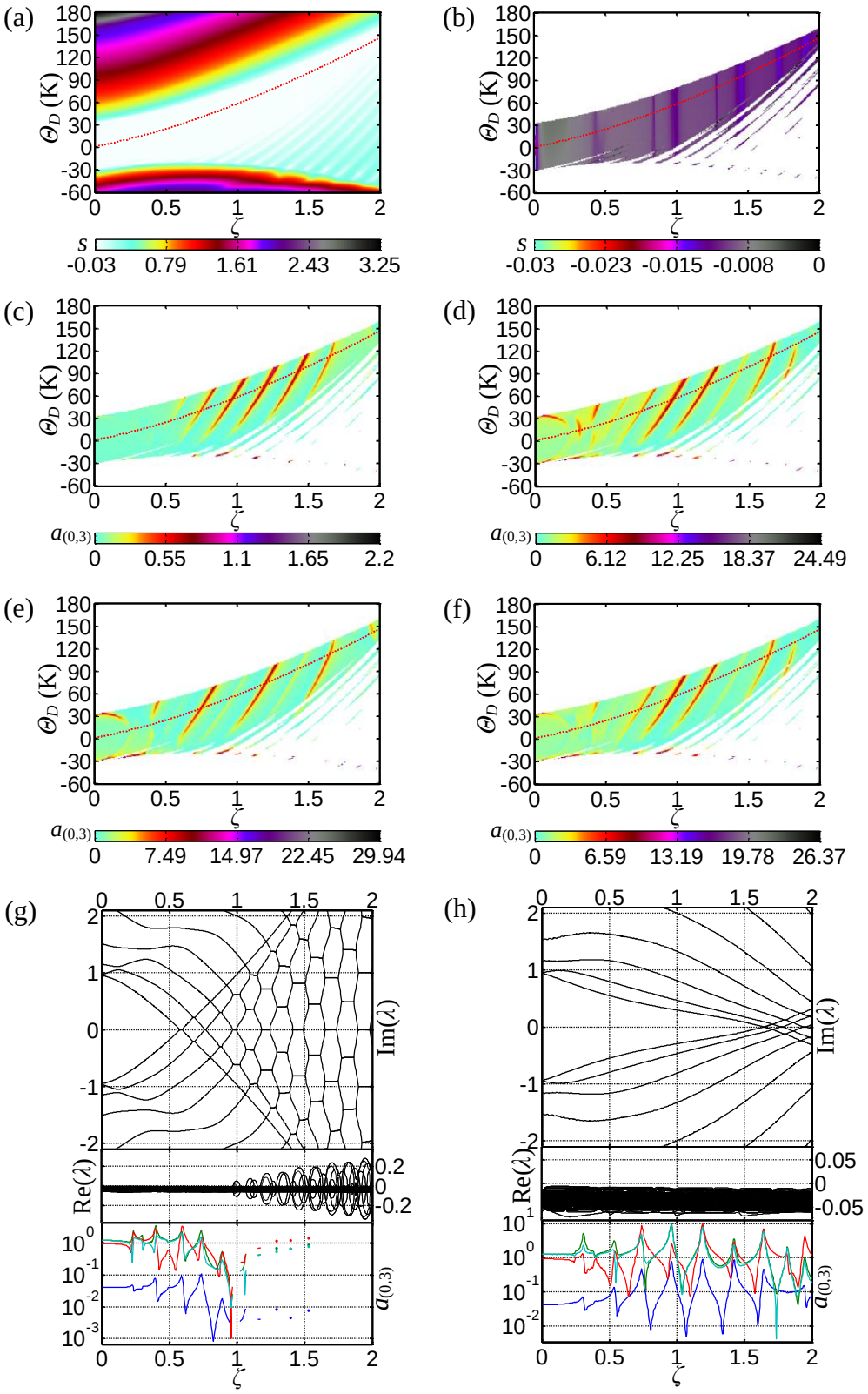

Fig.6 Dynamic characteristics of the rotating disk using shaft temperature increments for the case of slider mass m_s=0.01, disk air lift force χ=0 and slider spring initial deformation κ_F=0.02. Disk/slider configuration: Fig. 4(a). (a) Dynamic stability of the dimensionless disk rotational speed ζ - for shaft temperature increments Θ_D, ζ-Θ_D plane; (b) Stabilized region on ζ-Θ_D plane; (c) Steady state amplitude

$a_{(0,3)}$ on ζ-Θ_D plane: radial position r_P at disk outer edge a, circumferential position θ_P=0^o; (d) $a_{(0,3)}$: r_P=a, θ_P=90^o; (e) $a_{(0,3)}$: r_P=a, θ_P=180^o; (f) $a_{(0,3)}$: r_P=a, θ_P=270^o; (g) Eigenvalue λ and $a_{(0,3)}$ without temperature control; (h) Eigenvalue λ and $a_{(0,3)}$ with shaft temperature increment control $\underline{\Theta_D}(\zeta)$. In (a-f), Red dotted line: the assigned shaft temperature increment control $\underline{\Theta_D}(\zeta)$. In the nethermost subplot of (g-h), Blue line $a_{(0,3)}$: radial position r_P at disk outer edge a, circumferential position θ_P=0^o; Green line $a_{(0,3)}$: r_P=a, θ_P=90^o; Red line $a_{(0,3)}$: r_P=a, θ_P=180^o; Cyan line $a_{(0,3)}$: r_P=a, θ_P=270^o.

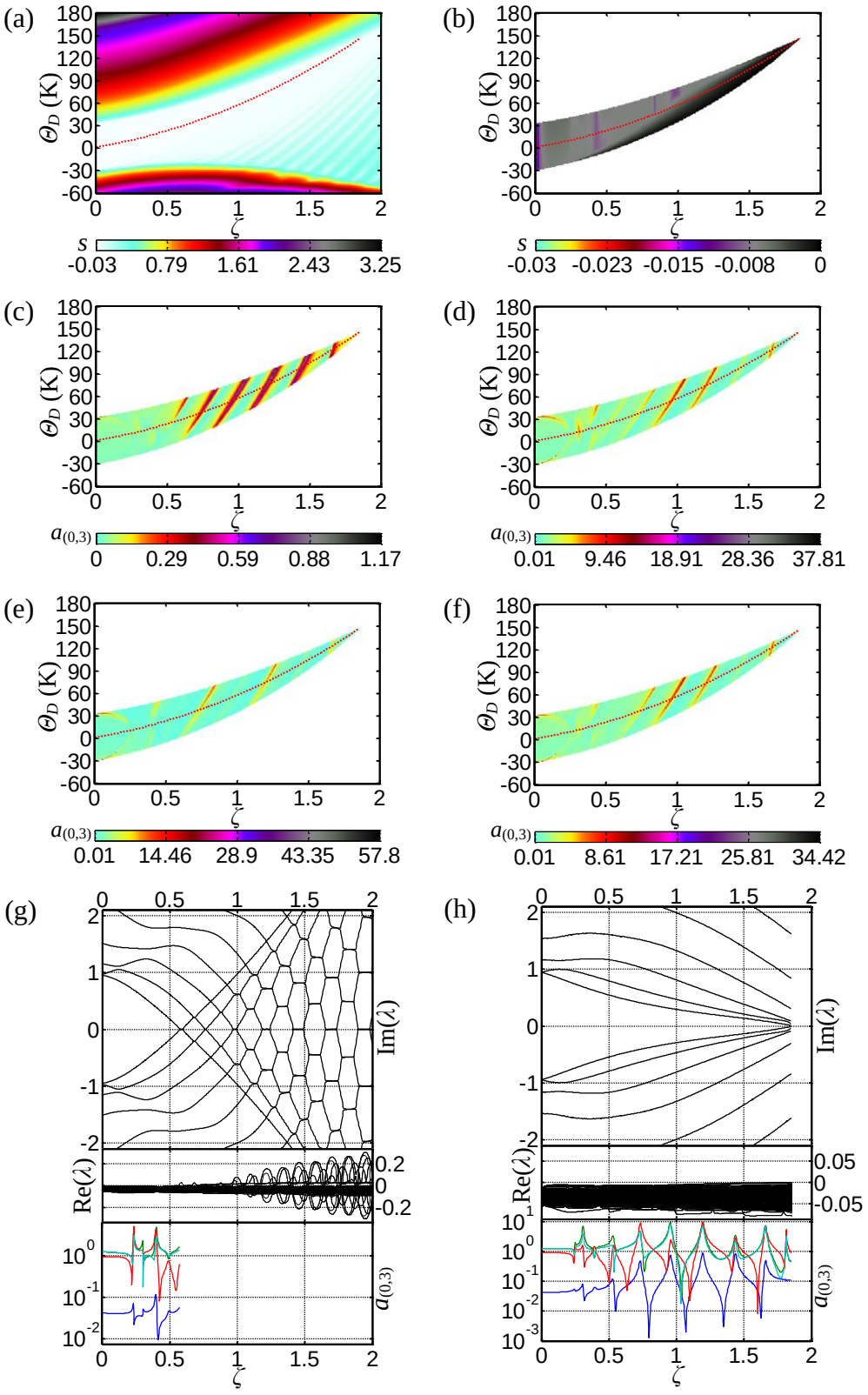

Fig.7 Dynamic characteristics of the rotating disk using shaft temperature increments for the case of slider mass m_s=0.01, disk air lift force χ=0.03 and slider spring initial deformation κ_F=0.02. Disk/slider configuration: Fig. 4(a). (a) Dynamic stability of the dimensionless disk rotational speed ζ - for shaft temperature increments Θ_D, ζ-Θ_D plane; (b) Stabilized region on ζ-Θ_D plane; (c) Steady state amplitude

$a_{(0,3)}$ on ζ-Θ_D plane: radial position r_P at disk outer edge a, circumferential position θ_P=0^o; (d) $a_{(0,3)}$: r_P=a, θ_P=90^o; (e) $a_{(0,3)}$: r_P=a, θ_P=180^o; (f) $a_{(0,3)}$: r_P=a, θ_P=270^o; (g) Eigenvalue λ and $a_{(0,3)}$ without temperature control; (h) Eigenvalue λ and $a_{(0,3)}$ with shaft temperature increment control $\underline{\Theta_D}(\zeta)$. In (a-f), Red dotted line: the assigned shaft temperature increment control $\underline{\Theta_D}(\zeta)$. In the nethermost subplot of (g-h), Blue line $a_{(0,3)}$: radial position r_P at disk outer edge a, circumferential position θ_P=0^o; Green line $a_{(0,3)}$: r_P=a, θ_P=90^o; Red line $a_{(0,3)}$: r_P=a, θ_P=180^o; Cyan line $a_{(0,3)}$: r_P=a, θ_P=270^o.

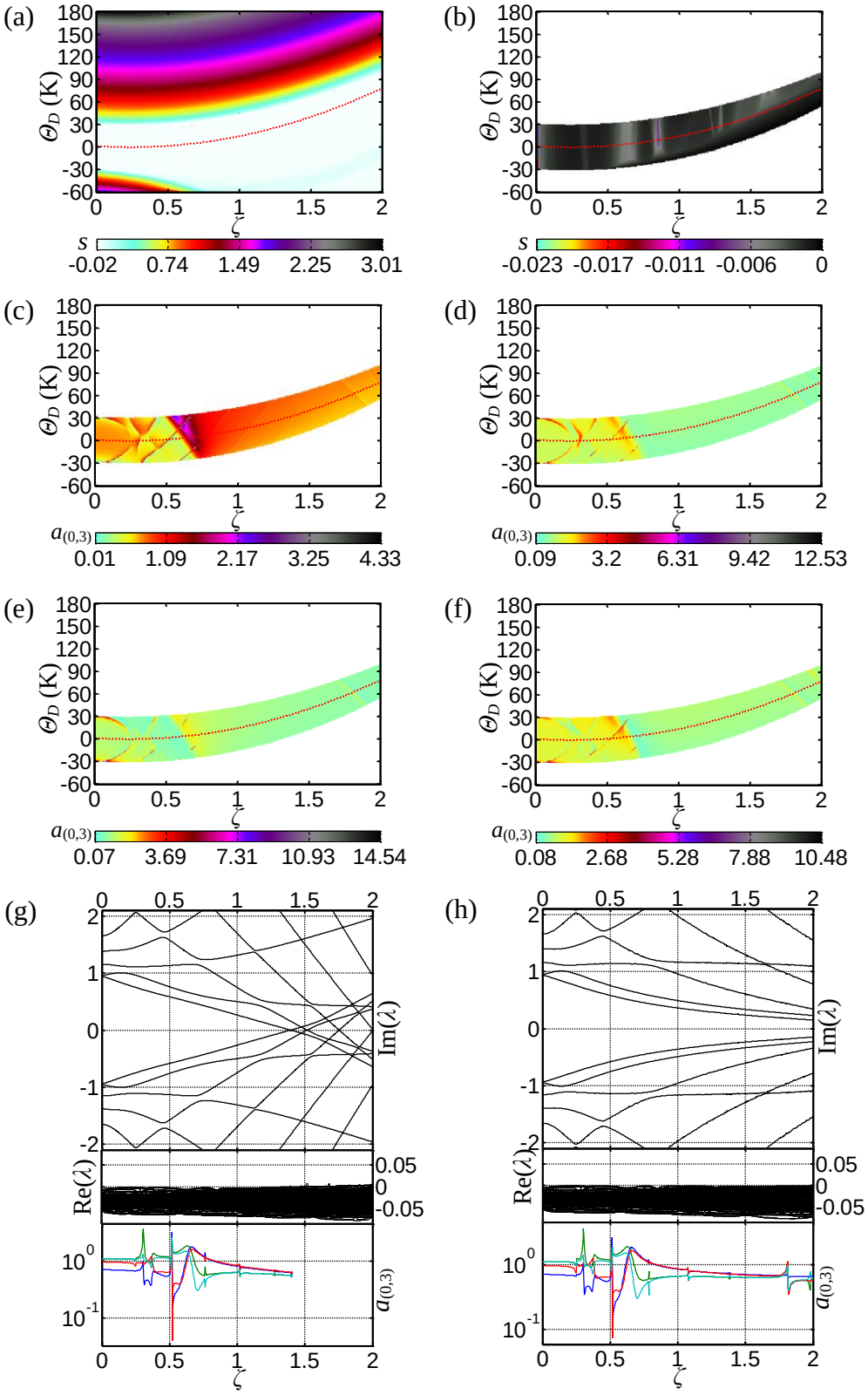

Fig.8 Dynamic characteristics of the rotating disk using shaft temperature increments for the case of slider mass m_s=0.01, disk air lift force χ=0.03 and slider spring initial deformation κ_F=0.02. Disk/slider configuration: Fig. 4(b). (a) Dynamic stability of the dimensionless disk rotational speed ζ - for shaft temperature increments Θ_D, ζ-Θ_D plane; (b) Stabilized region on ζ-Θ_D plane; (c) Steady state amplitude

$a_{(0,3)}$ on ζ-Θ_D plane: radial position r_P at disk outer edge a, circumferential position θ_P=0^o; (d) $a_{(0,3)}$: r_P=a, θ_P=90^o; (e) $a_{(0,3)}$: r_P=a, θ_P=180^o; (f) $a_{(0,3)}$: r_P=a, θ_P=270^o; (g) Eigenvalue λ and $a_{(0,3)}$ without temperature control; (h) Eigenvalue λ and $a_{(0,3)}$ with shaft temperature increment control $\underline{\Theta_D}(\zeta)$. In (a-f), Red dotted line: the assigned shaft temperature increment control $\underline{\Theta_D}(\zeta)$. In the nethermost subplot of (g-h), Blue line $a_{(0,3)}$: radial position r_P at disk outer edge a, circumferential position θ_P=0^o; Green line $a_{(0,3)}$: r_P=a, θ_P=90^o; Red line $a_{(0,3)}$: r_P=a, θ_P=180^o; Cyan line $a_{(0,3)}$: r_P=a, θ_P=270^o.